STATE OF ILLINOIS
DEPARTMENT OF REGISTRATION AND EDUCATION

IMPACT RESISTANCE OF ILLINOIS LIMESTONES AND DOLOMITES

Richard D. Harvey

ILLINOIS STATE GEOLOGICAL SURVEY
John C. Frye, *Chief*
URBANA

CIRCULAR 345
1963

IMPACT RESISTANCE OF ILLINOIS LIMESTONES AND DOLOMITES

Richard D. Harvey

ABSTRACT

The purpose of this study was to investigate the basic response of various textural types of relatively pure limestones and dolomites to a rapidly applied force (approximately 1 to 7 ft./sec.) and to determine a quantitative measure of the impact resistance of such rocks.

A simple instrument for determining the relative impact resistance of limestones and dolomites is described and the results of its use in testing 26 pure limestones of various textures and 10 dolomites are given. Analysis of test data indicates that the radius (r) of an indentation produced on a smooth carbonate rock surface is a function of the velocity (v) of impact of the indenter. The slope of the curve r^2 versus v is constant for carbonate rocks and its reciprocal may be termed the impact modulus of the material being tested. The impact modulus of limestones and dolomites decreases with increasing porosity and decreases with increasing size of the crystals within the rock. Although there is considerable scatter of data points, both relationships appear to be linear.

All of the limestones and dolomites tested deformed plastically immediately beneath the indenter by translation gliding. Fine-grained rocks reacted to impact primarily by the development of a distinct fractured zone around the point of indentation, whereas in coarse-grained limestones notable cleavage and $\{01\bar{1}2\}$ twinning of calcite took place in the area surrounding the indentation.

INTRODUCTION

The hardness of limestones and dolomites often varies considerably from one place to another, and it notably affects the commercial utilization of the stone. The term hardness as applied to solids is not always similarly defined, but it is agreed generally that it is a measure of the resistance to abrasion or deformation.

A variety of tests have been developed to measure hardness that involve various rates of application of load. Mohs' scratch test is used commonly by mineralogists to determine relative hardness of minerals, but this test is not sensitive enough to be used effectively on carbonate rocks. The Brinnell, Rockwell, and Vickers tests (Tabor, 1951), involving a slowly applied force that presses a spherical or pyramidal indenter into the sample, have been used effectively by metallurgists. Brace (1960), using the Vickers tester, showed that this test was applicable to the study of relatively isotropic and nonporous materials, including some limestones.

The results of strength tests of solids as measured under slowly applied load (static) are considerably different from those derived from impact or a rapidly applied load. Under static conditions stresses are generally distributed throughout the material, although they often become concentrated in certain regions. Under impact or dynamic conditions, stress pulses which travel through the solid are generated; thus, only a small portion of the material is stressed at any instant (of time), and it behaves essentially independent of neighboring portions. Thus, many solid materials, particularly brittle ones, appear stronger and harder under impact than under static conditions.

Limestones and dolomites undergo impact loading during crushing and drilling operations, when used as railroad ballast, in concrete highways, as road stone, and in other ways. In view of this, it was the general objective of this study to investigate the basic response of relatively pure Illinois limestones and dolomites to impact and to discover some of the phenomena that accompany impact of these rocks. As the limestones and dolomites of Illinois are similar to such rocks in other places, it is thought that the results of the study will be of general significance.

A review of the literature on impact testing of materials reveals that several methods have been developed. Greaves (1909) measured the relative height of rebound of a diamond-tipped hammer falling freely on various metal surfaces (scleroscope hardness), and Gilbert (1954) determined the scleroscope hardness of single crystals of the Mohs' scale minerals. A "cloudburst" machine developed by Herbert (1929) subjects the surface of a material to a rain of hard steel balls falling from a known height. Studies have been made of materials subjected to impact by high velocity projectiles (Whiffin, 1948; Maurer and Rinehart, 1960; and others). Obert et al. (1946) and the Page toughness test (A.S.T.M., 1961) determine impact toughness of rocks by dropping a hammer from continuously increasing heights until the specimen breaks. Impact tests in which a pendulum applies a load sufficient to break the material are described and discussed by Späth (1961). Singh and Hartman (1961) used an impact device consisting of a weighted chisel about one inch wide which was dropped from various heights on specimens of granite and limestone.

Application of these and other tests to carbonate rocks is limited in one way or another, and it was thought that a simple impact apparatus utilizing a spherical indenter dropped vertically on a smooth rock surface would provide additional and useful information. The specific purposes of this investigation were to devise an apparatus and procedure for measuring impact resistance of limestones and dolomites that could be used to arrive at a numerical means of expressing this hardness, to evaluate the effect of impact on different textural types of relatively pure limestones and dolomites, and to determine the relation of impact hardness to other physical properties.

Acknowledgments

Thanks are extended to J. E. Lamar, R. J. Helfinstine, and J. S. Machin of the Illinois State Geological Survey for their assistance and discussions during the course of this investigation, and to D. U. Deere and E. Y. Huang of the University of Illinois for their critical reading of the manuscript.

IMPACT HARDNESS TESTER

Description of Indenter

The apparatus used in the present study consists of an indenter made of a 3/8 inch diameter steel rod, with a 5/32 inch diameter hardened steel sphere attached to its tip, that falls vertically upon the sample being tested. Figure 1 is a diagram of the apparatus drawn to scale. The height of fall of the indenter is indicated by an attached pointer, the tip of which moves in a groove in a meter stick fastened to the supporting frame. A spring loaded pawl, which is mounted on the indenter, is released when the indenter strikes the sample. The pawl engages a ratch at the highest point of indenter rebound, thereby preventing the indenter from striking the sample a second time. The tip of the pointer prevents the rod from rotating during its fall and thus assures that the pawl is oriented properly. The indenter rod moves vertically through two laterally adjustable guides that are machined to allow the rod to touch them only on a very small area. The sample is clamped on an adjustable table to insure that the indented surface is perpendicular to the indenter. The entire apparatus is securely mounted on a sturdy laboratory bench.

The kinetic energy of the indenter as it strikes the sample is equal to its potential energy at height h above the sample minus the frictional energy encountered during the fall. The energy E of impact in ergs is, therefore,

$$E = mgh - fh \qquad (1)$$

where m is the mass of the indenter in grams, g is the gravitational acceleration (980 cm/sec^2), h is the height of fall in cm, and f is the force of friction encountered during the fall. The second term on the right side of (1) is the total work done or energy expended against friction. The friction is given by

$$f = \mu N$$

where μ is the coefficient of friction and N is the fraction of the mass of the indenter that makes contact with the bearings and between the pointer and the sides of the groove in the meter stick during the fall. The static coefficient of friction in this case is approximately 0.2 and the kinetic coefficient would be even less (Fairman and Cutshall, 1946); however, N is not known. It is reasonable to assume that N would be less than 10 percent of the total weight of the indenter and would approach 0 when the guides are in perfect alignment. Even with a value of 63.2 for N (10 percent of the weight of the indenter), 0.2 for μ, and 10 cm fall for h, the frictional loss is 130 ergs. The potential energy with a 10 cm fall is 61.9 x 10^5 ergs, or approximately 48,000 times the friction loss under these assumed extreme conditions. Thus, friction during the fall may be neglected in this study.

The velocity of a freely falling body which is initally at rest is given by

$$v = gt \qquad (2)$$

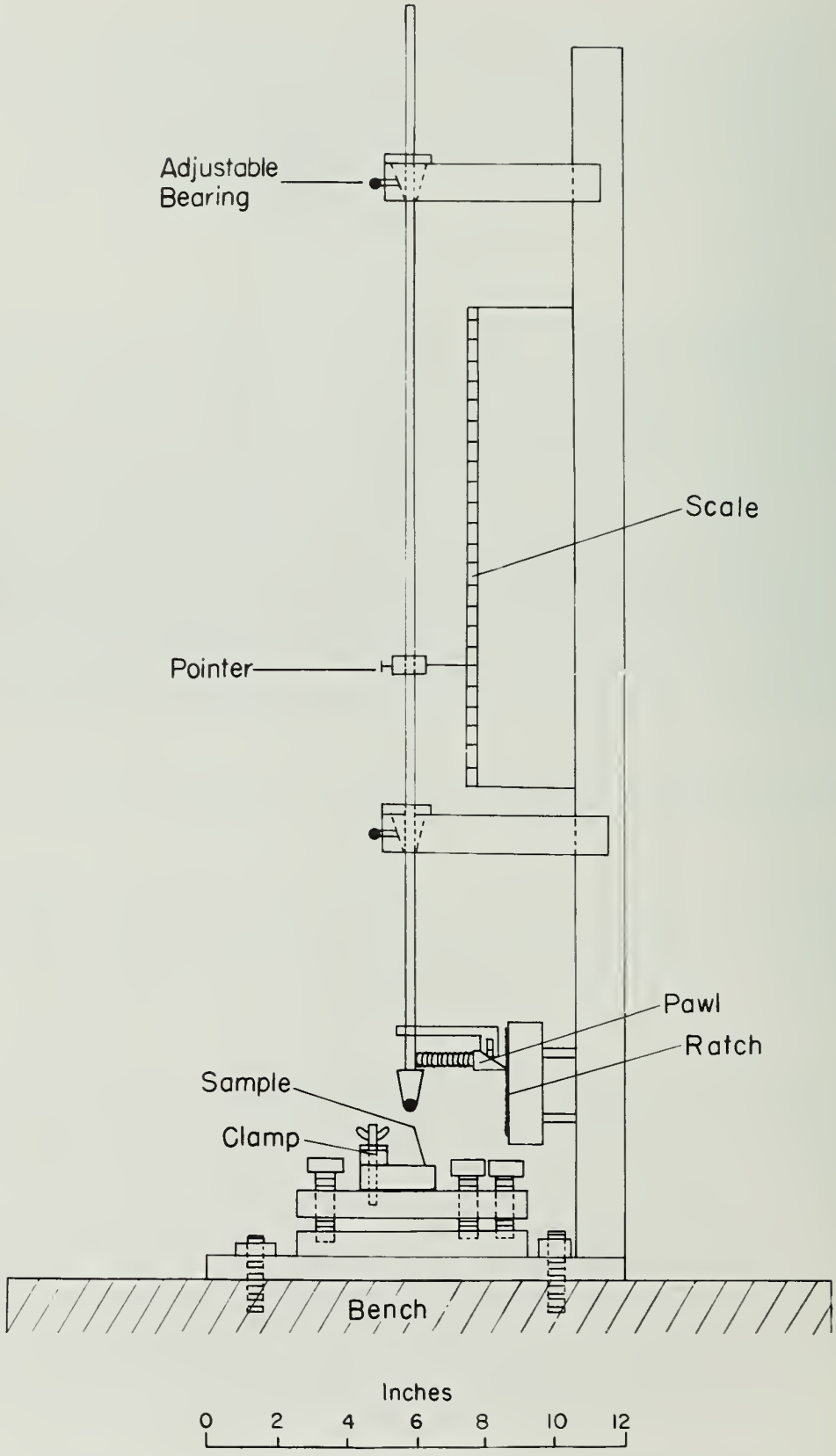

Fig. 1 - Diagram of indenter shown in a rest position after indentation of sample.

where t is the time duration of fall. Since

$$\frac{dh}{dt} = v$$

$$h = \int_{t=o}^{t=t} gt\, dt = \frac{g\, t^2}{2}$$

and the time of fall is thus

$$t = (2\, h/g)^{\frac{1}{2}}.$$

From (2) the velocity in cm/sec is

$$v = (2gh)^{\frac{1}{2}} = 44.27(h)^{\frac{1}{2}}. \qquad (3)$$

Testing Procedure

The samples for impact hardness tests were blocks of limestone and dolomite, approximately 2 x 2 x 3/4 inch, sawed and ground so that their 2 x 2 inch surfaces were smooth and essentially parallel to each other and to the bedding of the stone. No notable differences were obtained in a test series of blocks of variable thickness cut from the same limestone sample. Some blocks thinner than 3/4 inch broke during impact tests and were deemed unsuitable. A slight polish was put on one of the 2 x 2 inch faces and the indentation tests made on this face. Although there was a slight amount of work hardening detected, the polish facilitated accurate measurements of the indentations and did not materially affect the relative results of the tests.

The sample was clamped to the adjustable table and leveled; the indenter was raised by hand to the desired height and released. After striking the sample, the indenter rebounded and was caught by the pawl and ratch. The sample was then moved about 1 centimeter or more and the operation repeated to produce another dent. The amount of rebound of the indenter was highly dependent on the action of the pawl and ratch. The tip of the pawl underwent some wear after prolonged use, and thus the friction encountered during rebound was not absolutely constant for each test. Therefore, the observed height of rebound did not truly reflect a characteristic property of the test sample.

Measurements of Indentations

The diameter of each indentation was measured by means of a vertical illumination microscope to the nearest 0.01 mm. The depth of indentation was measured using a hard blue dental inlay casting wax to make a cast of the impression. The cast was sectioned with a razor blade so that the maximum depth of the indentation could be measured with a microscope. Any plastic deformation of the wax mold due to sectioning with the razor was easily recognized. The depths of the indentations were determined to the nearest 0.01 mm.

Reproducibility of Indentation Diameter

Numbers of Indentations Required

The reproducibility of the indentation diameter made in any single test block was evaluated in the following manner. Specimens of coarse-, medium-,

and fine-grained limestones were indented 10 times each using an indenter fall of 6 centimeters. The average diameter of 3, 5, and all 10 indentations are shown in table 1, together with their respective standard deviations and limits for the mean (Bennett and Franklin, 1954, p. 28). Measurements of the diameter of 5 indentations spread over the surface of the sample were regarded as adequate for the test. Standard deviations based on 5 indentations computed for samples used in this study, other than coarse-grained ones, were equal to or less than 0.05 mm. Sample C2740 (table 1) gave the largest standard deviation of all the samples tested.

Consistency of Indentation Results

The variation in average indentation diameter of several test specimens cut from large single blocks of limestone was investigated for 13 such blocks, each representing a different type or stratum of limestone. Results of such tests are shown in table 2; textural and other characteristics of the samples mentioned are described subsequently. In general the results show a good consistency, and such variations as exist occur when limestones have a highly variable texture.

IMPACT MODULUS

Indentation tests were made on more than 36 different limestones and dolomites. Tests were made in which the height of fall varied from 1 to 10 cm for the limestones and 2 to 20 cm for the dolomites. The corresponding velocity of impact according to (3) is 44.3 to 140.0 and 62.6 to 197.9 cm/sec. Graphs of the square of the indentation radius (r) plotted against the impact velocity for several different types of limestones and a dolomite are shown in figure 2. Although there is some scatter of the points, they clearly indicate that r^2 is a linear function of the indentation velocity. This relation also was found true for impact craters in granite and sandstone produced by projectiles with velocities from 1000 to over 6000 feet per second (Maurer and Rinehart, 1960). Extrapolation of the lines in figure 2 to zero velocity indicates they all pass through the origin, or nearly so, and thus an equation in the form,

$$100r^2 = \left(\frac{1}{K}\right)v \qquad (4)$$

where K is the reciprocal of the slope of the curve and v the velocity appears to predict satisfactorily the behavior of carbonate rocks using this impact tester. The units of K are 1/(cm-sec.) when the height of fall and the radius of indentation are in cm. Of all the rocks tested, K ranges from 77 to 422 units (see table 5). Variations in K computed from specific values of r and v as v varies from 44.3 to 197.9 cm/sec. for several carbonate rocks are shown in figure 3. The average maximum difference in K for seventeen different carbonate rocks is 16 units. Some rocks show a maximum difference in K as small as 10 units which represents a maximum of 5 percent variation, and others such as K14 show a maximum difference of 36 units, which represents a maximum of 14 percent variation in K. These percentage variations are not unusual for measurements of mechanical properties of natural occurring rocks. Thus, for a rapid and relative determination of the impact resistance of carbonate rocks, the average diameter of at least 5

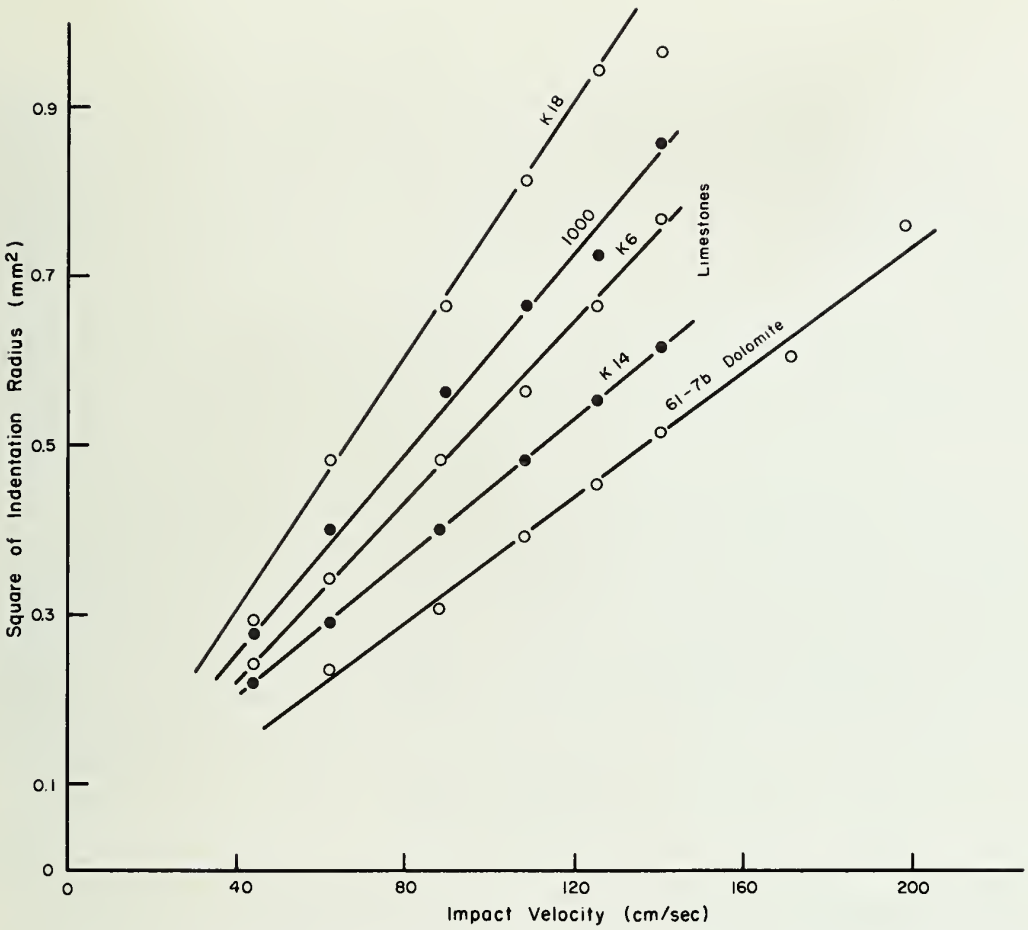

Fig. 2 - Square of indentation radius versus final impact velocity for several limestones and a dolomite.

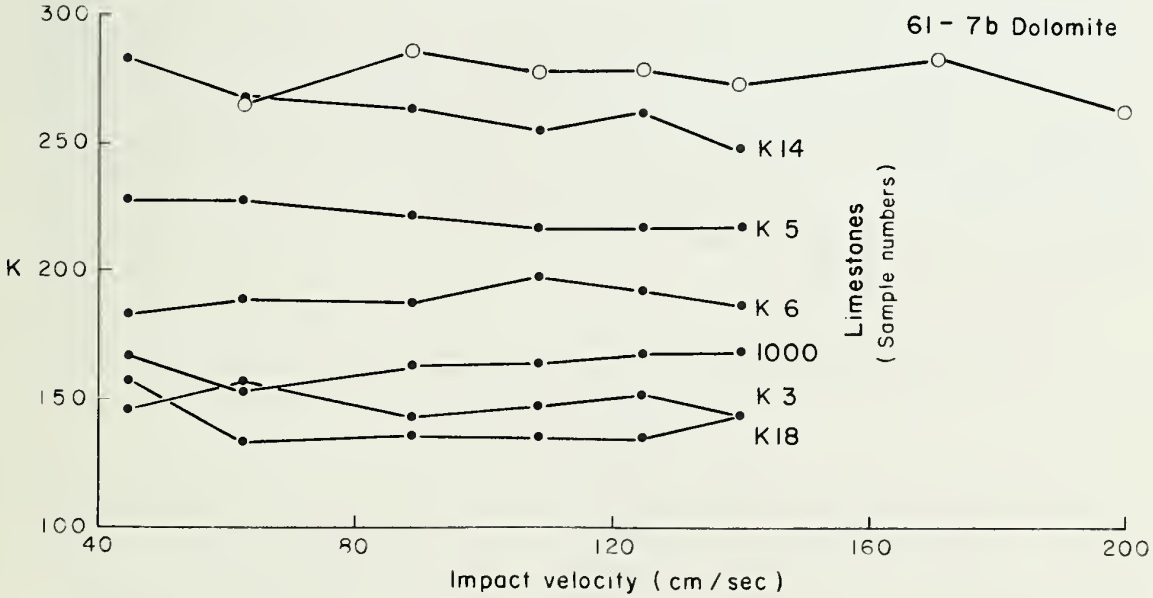

Fig. 3 - Variation of K computed from results obtained using various impact velocities for several limestones and a dolomite. See table 4 for description of samples.

indentations, produced by impact of the indenter dropped from a selected height, yields a characteristic value K to which the term impact modulus is applied.

The indentations produced by a fall of 2 cm or less were too small to be observed readily in some samples. A fall of 10 cm caused ejection of some of the grains from around the indentation in many limestones and, hence, made measurements of the size of the indentation somewhat unsatisfactory. The standard deviation of K for sample K 14 (table 1) is 3.1 units and for C2740 it is 24 units. The adoption of K as a quantitative measure of the impact hardness or resistance to impact of carbonate rocks enables comparison of results from rocks having a grossly different behavior and resistance to impact.

INDENTER REBOUND AND ELASTIC RECOVERY OF ROCK SAMPLE

When the indenter strikes a test block, it rebounds to varying heights depending mainly on its height of fall and the physical properties of the sample. The elasticity of individual calcite crystals at the site of an indentation enables the limestone to return partly to its position prior to impact. The depth of the resulting indentation, therefore, is less than the actual amount of penetration by the indenter. It is reasonable to assume that the maximum elastic rebound of the limestone would be in the center of the indentation and the minimum at the edge. The indenter point also undergoes some elastic deformation during impact. This is thought to be small as compared to that of the limestone because the elastic modulus (Young's modulus) of hardened steel is about 4 to 7 times that of limestone.

Taking into account the foregoing, a relative value for the amount of recovery of a limestone can be obtained as the difference between the maximum measured depth of an indentation, D_m, and a depth, D_c, calculated from the diameter of the indentation and the radius of the indenter as follows:

$$D_c = R - (R^2 - r^2)^{\frac{1}{2}}$$

where R is the radius of the indenter (1.985 mm) and r the radius of the indentation.

The amount of elastic recovery of selected limestone samples in millimeters and in percent of the maximum indentation is shown in table 3. The elastic recovery shown is thought to be mainly that of the limestone, although a small part of the recovery may be due to flattening of the indenter point at the time of impact so that the indentation is larger than it would be otherwise. There is no apparent relation between the percentage of elastic recovery of the limestone and its impact modulus.

APPLICATION OF IMPACT TEST TO LIMESTONES AND DOLOMITES

Description of Samples

The impact modulus of 26 limestones consisting essentially of calcite and 10 "pure" dolomites was determined according to the procedures previously described. Among the samples were limestones having a wide range of textual variations, including exceedingly fine-grained, lithographic types; medium-grained but finely crystalline oolites; and medium- and coarse-grained bioclastic limestones.

X-ray and microscopic analyses of indented surfaces indicate many of the limestones are completely free of detectable quartz, dolomite, and other impurities.

Of the limestones reported in this study (see table 4) only samples NF512, NF511, NF527, 1009, and K19 have noteworthy amounts of impurities consisting of dolomite and/or quartz grains, but these grains are dispersed so thinly that they do not noticeably affect the impact modulus. No calcite was detected in any of the dolomites studied; however, samples 62-16-1, 62-16-2, and 61-7b contain a few widely scattered grains of quartz.

Most of the fossil fragments in the limestones studied are parts of crinoids and bryozoans. The crinoid fragments are commonly single crystals; whereas, the bryozoan fragments are very fine-crystalline aggregates, usually fibrous, consisting of many individual crystalline particles whose orientation differs from its neighbors by a very low angle. The oolites are rounded grains composed of one or more rings of very fine polycrystalline calcite and usually possess a nucleus of one or more calcite crystals whose size is much larger than those in the outer rings.

For descriptive purposes, the limestones are classified (table 4) accordingly: (1) type of major constituents (classification of Folk, 1959), (2) grain size grouped into fine, medium, and coarse categories according to the average clastic particle being < 0.063 mm as fine, 0.063 to 1.0 mm as medium, and > 1.0 mm as coarse (modified from Folk, 1959). In the case of dolomites, it was useful to consider the medium range from 0.063 to 0.25 mm. Critical remarks based on microscopic analysis also are included in the table.

Nature of Deformation

Fracture Patterns

Striking differences are evident in the behavior of limestones subjected to impact forces as applied in the test. All the dolomites behaved similarly and in much the same way as the fine-grained limestones. Impact on fine-grained limestones and dolomites developed indentations with sharp edges and narrow upheaved rims that stand approximately 0.005 mm above the surface of the rock, figure 4. Coarse-grained limestones, however, developed indentations whose edges are much less sharp and surrounded by a light colored upheaved zone in which complex deformation had occurred. The light colored zone consists of cleaved, twinned and buckled crystalline particles which were forced free of the rock in a few places as illustrated in the top of figure 5. By comparison the fine-grained limestones show only simple fracturing, and crystals adjacent to and surrounding the fractures and indentation have not suffered notable deformation. Medium-grained limestones composed of oolites and finely crystalline fossil fragments, such as bryozoans and brachiopods, behaved as fine-grained limestones, although a few oolite grains buckled and otherwise behaved as a unit during impact tests. Medium-grained limestones consisting of a few coarsely crystalline crinoid fragments with a fine-grained matrix show characteristics of both types of fracturing and deformation depending upon which type of material the indenter strikes.

Two types of fractures that develop during impact are recognized, (1) radial fractures extending outward from the dent, and (2) fractures approximately 0.8 to 1.0 mm beneath and essentially parallel to the surface of the specimen. Both types are most clearly observed in fine-grained limestones as illustrated in figure 6; however, in coarse-grained specimens these fractures appear to be present but their patterns are more obscure and complex. In the coarse specimens, the interaction of both types of fractures gives rise to the buckling and the light colored zone described above. The parallel fractures split into numerous subparallel

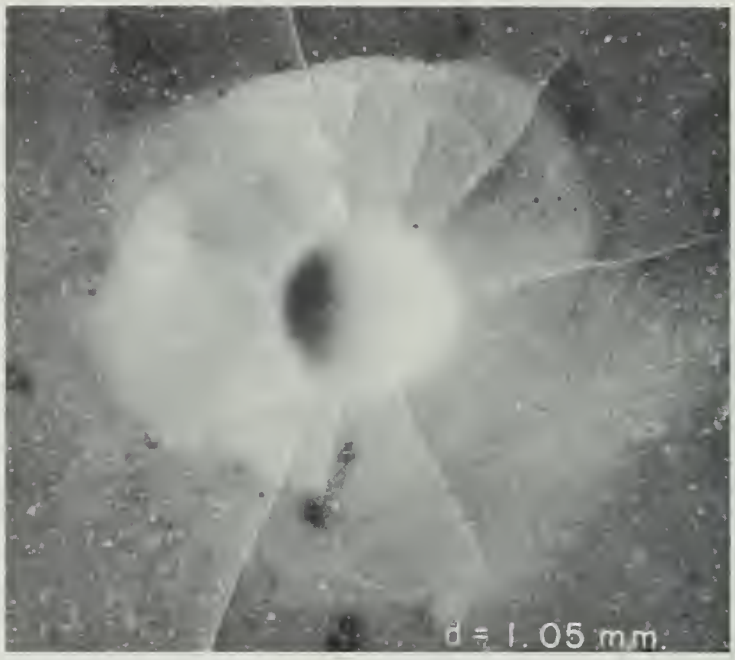

Fig. 4 - Photograph of an indentation in reflected light showing characteristic fracture pattern of fine-grained limestones. Light is shining from left to right and "d" is the diameter of the indentation.

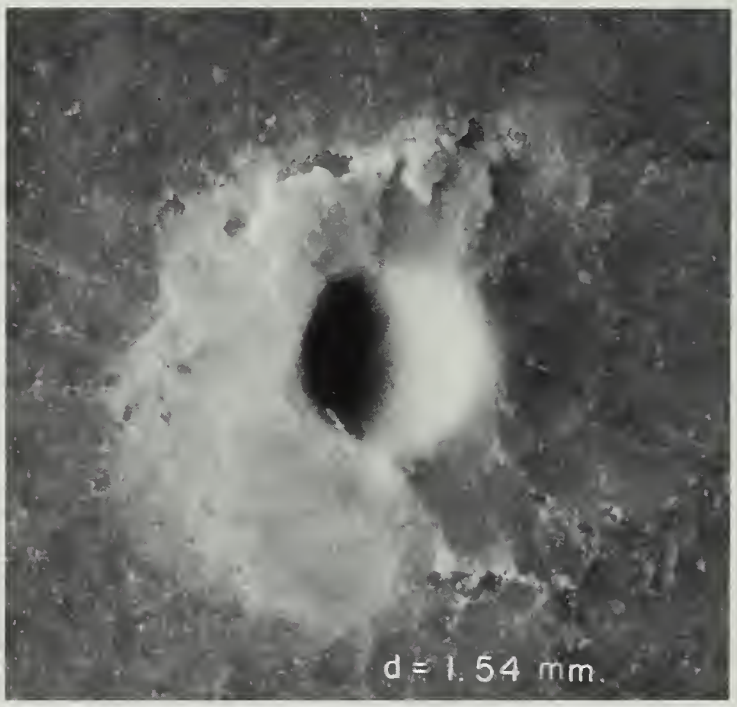

Fig. 5 - Photograph of an indentation in reflected light showing characteristic fracture pattern of coarse-grained limestones. The light is shining from left to right and "d" is the diameter of the indentation.

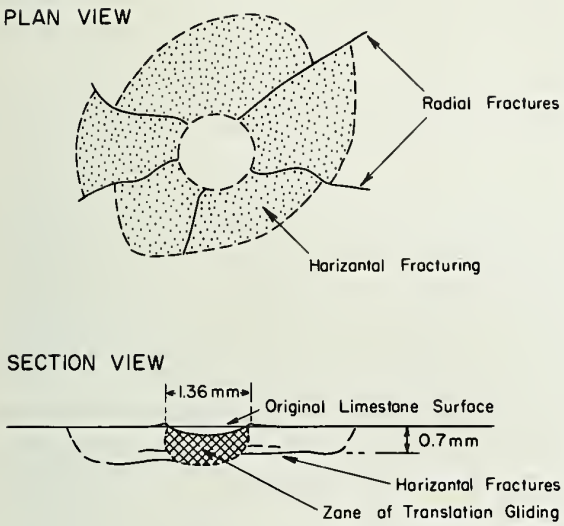

Fig. 6 Diagram of plan and section view of an indentation in fine-grained (sublithographic) limestone.

fractures which intersect the radial fractures, thereby isolating many particles. Radial fractures tend to follow grain boundaries, and thus their trace on the surface of the specimen is nearly a straight line in fine-grained and very irregular in coarse-grained limestones (compare figure 4 and 5). Radial fractures generally extend further in fine-grained than in coarse-grained rocks, which is probably related to the grain boundary phenomenon just mentioned. Inspection of fracture patterns, particularly in fine-grained specimens, shows that the terminating arcs of the parallel fractures are bounded by radial fractures as shown in the plan view of figure 6. This indicates that the radial fractures preceded the formation of the parallel fractures.

Crystal Deformation

Many of the individual crystals in the limestones and dolomites were deformed at and near the point of impact. According to Handin et al. (1957), calcite crystals that have undergone translation gliding (slip) on $\{10\bar{1}1\}$ crystallographic planes develop color centers which give the crystal a blue color after irradiation. It was found, as did Brace (1960) and Pavlova and Shreiner (1961), that indented areas in which translation gliding took place could be recognized by this blue color after irradiation with unfiltered Cu radiation for a period of one hour at 35 kv-18 ma imput to the x-ray tube. By placing the indented specimen 3 to 5 cm from the x-ray source, good results were obtained.

The calcite crystals of limestones yielded plastically by translation gliding within a segment of a spheroid immediately below the area of contact with the indenter and some distance into the specimen. By sawing through the middle of an indentation and irradiating the cross section of the indentation, the maximum depth to which the translation gliding took place could be measured (see section view in figure 6). The depth to which translation gliding took place appeared to increase gradually from approximately 0.1 to 1.0 mm with increasing impact velocity from 44.27 to 139.98 cm/sec. Maximum depth of this gliding for several limestones varies from 0.72 to 0.93 mm with an impact velocity of 125.2 cm/sec. These depths do not appear to be related to the measured indentation diameters of the different limestones. Generally, the blue color extended a few hundreths of a millimeter below the parallel nearly horizontal fractures. Close examination of irradiated indentations revealed that color centers were absent along planes that had cleaved and that larger crystals tended to be a deeper blue than smaller ones. The blue color disappeared when the sample was heated to 200° C.

Dolomite crystals located within the indentation also developed blue color centers as a result of the impact. Correlation between color centers and crystallographic mechanisms of deformation observed in dolomite crystals has

not been investigated to date; however, dolomite is known to slip on $\{0001\}$ only (Higgs and Handin, 1959), and thus it is thought that the color centers are formed as a result of dislocations or vacancies produced along $\{0001\}$ during impact.

Deformation lamellae were observed on surfaces of many crystals in the rock surrounding the zone of translation gliding in limestones. Twin lamellae produced by impact were not observed on dolomite crystals. According to Higgs and Handin (1959, p. 275), dolomite crystals do not twin at room temperature. Examination of thin sections of indented limestone surfaces using a polarizing microscope equipped with a universal stage revealed that the lamellae in calcite crystals resulted from lamellar twinning on $\{01\bar{1}2\}$ and cleavage on $\{10\bar{1}1\}$. A small number of crystals had lamellae parallel to $\{02\bar{2}1\}$ in this zone. The latter lamellae, according to Turner et al. (1954, p. 909), are a result of translation gliding rather than twinning. No detailed measurements of the orientation of the $\{01\bar{1}2\}$ twinning were made, but it was observed that such lamellae were preferentially oriented in such a way that a line drawn from the center of the indentation would intersect the lamellae at angles near 90 degrees. Figure 7 is a photomicrograph of part of an indentation and surrounding area in reflected light. It is a rare example that shows twin lamellae only in crystals located some distance from the indentation. This indicates that either the crystals adjacent to the dent just happened to be improperly oriented so that neither twinning nor cleavage could take place, or that the primary and secondary elastic waves generated by the impact interacted in a way to reenforce each other to produce deformation in a curved zone, as in figure 7. In addition,

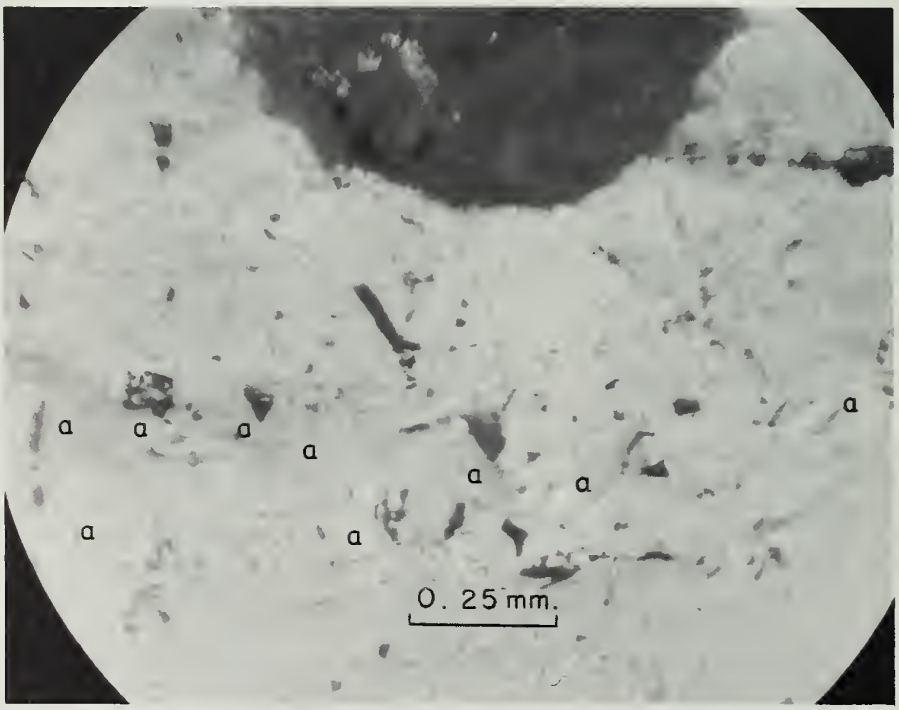

Fig. 7 - Photomicrograph of part of an indentation as seen from above in reflected light showing twin lamellae $\{01\bar{1}2\}$ on crystals (a) some distance from the indentation. Note that crystals adjacent to the indentation are untwinned.

this zone is located in the position where the parallel fractures generally intersect the surface.

RELATION OF IMPACT MODULUS TO POROSITY AND CRYSTAL SIZE

Data relating the strength of carbonate rocks to other physical properties are limited. From static tests on five nonporous limestones, Brace (1961) concluded that Vicker's hardness is related to the strength and maximum grain size of the rock. Finogenov (1958) using a similar test showed that the hardness of argillaceous carbonate rocks increased with increasing carbonate content and decreased with increasing porosity.

Absolute porosity measurements reflect the macro- and microscopic imperfections of limestones, dolomites, and other solid materials. The fact that these imperfections, as well as crystal imperfections such as dislocations, vacancies, and interstitial ions, etc., largely determine the mechanical properties of solids is well known (Mott, 1952; Evans and Pomeroy, 1958; and others); but many problems that relate the interactions of these imperfections with specific polycrystalline solids remain.

The impact modulus of the carbonate rocks described above was determined with the results listed in table 5. The modulus ranged from 77 to 275 for limestones and 149 to 422 for the dolomites. The effective porosity of each indented block was determined from water absorption and bulk volume displacement measurements, and the results are shown in table 5. Effective porosity ranges from 0.01 to 17.3 percent. The absolute porosities are undoubtedly slightly higher than these apparent values; nevertheless, relations between impact modulus and porosity should be evident from the data.

A plot of K versus effective porosity for limestones and dolomites (fig. 8) shows a linear decrease in K as the porosity increases for both rock types. The data for the limestones has been divided into two groups to show the relation between K and porosity for specimens with similar median crystal size (see below). The slope of the curves joining points of similar crystal size appears to increase slightly as the crystal size decreases.

Crystal particle size distribution of the limestones was determined from thin section analysis by the point count method (Friedman, 1958). The apparent maximum dimension of 100 or more individual crystalline particles located on a grid covering approximately 6 sq. cm. of rock was grouped into 11 size ranges. Cumulative frequency curves were constructed from the data and the quartile distribution sizes obtained are listed in table 5. Q_1, M_d, and Q_3 correspond, respectively, to that crystalline particle size for which 75 percent, 50 percent, and 25 percent of the particles are larger than the value given in the table.

When the logarithm of M_d (median) is plotted against K for limestones which have an effective porosity of less than 4 percent, figure 9, a linear trend of increasing K with decreasing M_d is evident, although there is considerable scatter to the points. The Q_1 and Q_3 values of the samples when similarly plotted give much the same trend but the scatter of points is slightly greater. As a result of the small differences in the median crystal size of the dolomites, a plot of K versus M_d for these rocks does not show a significant trend.

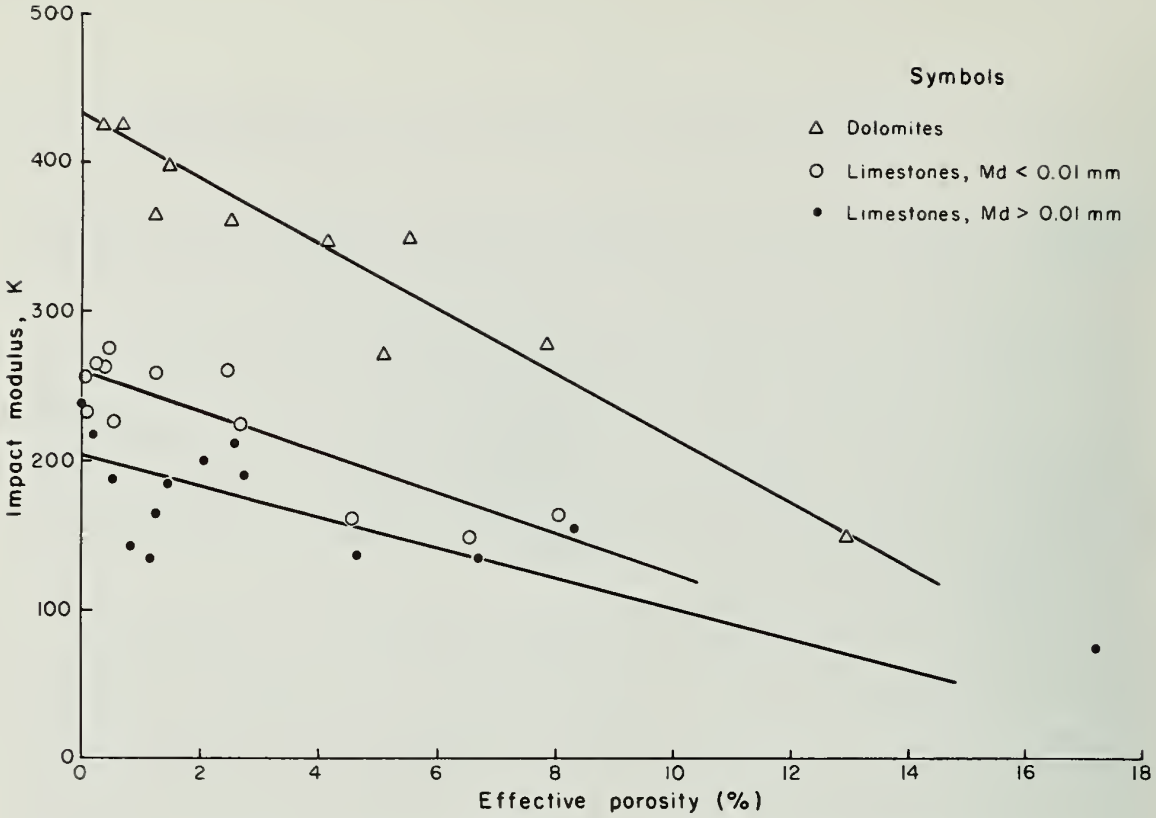

Fig. 8 - Impact modulus versus effective porosity for pure limestones and dolomites.

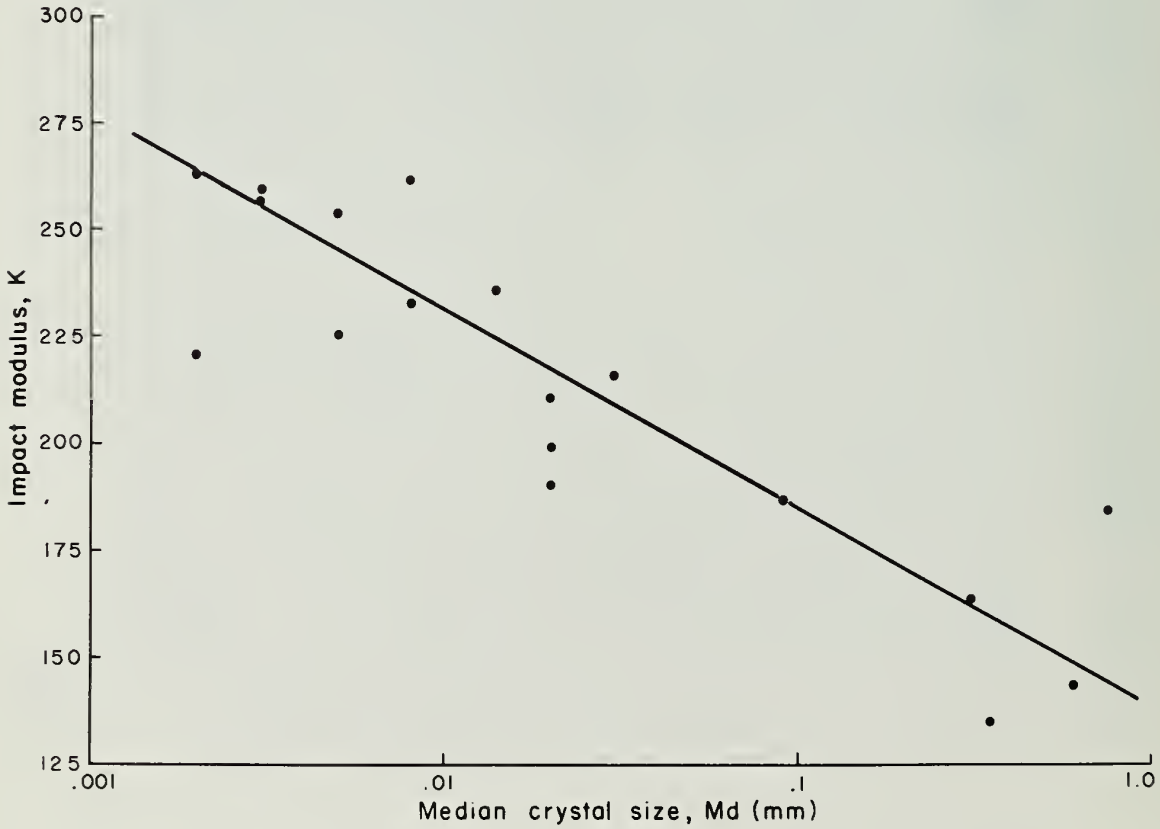

Fig. 9 - Impact modulus versus median crystal size for limestones with effective porosity less than 4 percent.

CONCLUSIONS

A simple and rapid test has been devised to determine the ability of carbonate rocks to resist deformation by impact. The equation

$$r = \left(\frac{v}{K}\right)^{\frac{1}{2}},$$

where r is the average radius of at least 5 indentations produced by impact of a spherical indenter of velocity v and K is a constant characteristic of the material, quantitatively describes the behavior of carbonate rocks subjected to impact. This equation was evaluated only for cases in which v ranged from approximately 40 to 200 cm/sec., thus the boundary conditions for the equation have not been defined. It is proposed that the term impact modulus be applied to K. The units of K are 1/(cm-sec), provided that the radius and distance of fall of the indenter are measured in cm. The impact modulus ranges from 149 to 422 for 10 pure dolomites and 77 to 275 for 26 pure limestones.

Impact penetration of carbonate rocks by a spherical indenter produces well-defined zones of plastic and brittle deformation. An indentation is formed by translation gliding on the $\{10\bar{1}1\}$ in calcite and $\{0001\}$? in dolomite crystals and by compaction of crystals in the case of porous rocks. A zone in which cleavage on $\{10\bar{1}1\}$ and lamellar twinning on $\{01\bar{1}2\}$ takes place on individual calcite crystals surrounds the indentation. This zone has a diameter roughly equal to twice the diameter of the indentation and includes an upheaved area adjacent to the dent, which varies in height and width depending on the texture of the rocks. Lamellae parallel to $\{02\bar{2}1\}$ also were observed microscopically in calcite crystals in this zone near the rim.

Impact on coarse-grained limestones produces a considerably wider and higher upheaved area than on fine-grained stones. Cleavage and twinning of crystals, and buckling up of crystalline fragments by fracturing along grain boundaries are predominately observed on coarse-grained limestones. If the impact velocity is sufficient, small particles of stone from the outer margins of the deformed zone may be exploded free from the surface of the specimen. Fine-grained limestones and dolomites, on the other hand, show little crystal deformation adjacent to the indentation.

Two types of fractures are evident and most clearly observed in fine-grained limestones. One set of fractures radiates from the indentation rim; the other set is located approximately 1 mm beneath and nearly parallel to the surface of the sample immediately beneath the indentation, but it turns to intersect the surface some distance from the dent. These limiting characteristics of coarse- and fine-grained rocks also are developed in medium-grained limestones but to a more limited extent.

The resistance to impact of relatively pure limestones and dolomites is, for the most part, controlled by the porosity and size of the crystals composing the rock.

TABLE 1 – NUMBER OF INDENTATIONS AND THE LIMITS OF THE MEAN DIAMETER

Number of dents	Mean diameter (in mm)	Range for 10 dents (in mm)	Standard deviation (in mm)	Limits of the mean* (in mm)
Coarse-grained limestone (C2740)				
3	1.720		0.140	0.35
5	1.830		0.179	0.22
10	1.808	1.62–2.02	0.172	0.12
Medium-grained limestone (K7)				
3	1.537		0.025	0.06
5	1.536		0.025	0.03
10	1.541	1.51–1.56	0.023	0.02
Fine-grained limestone (K14)				
3	1.313		0.014	0.03
5	1.310		0.010	0.01
10	1.308	1.305–1.330	0.006	0.004

* Based on 95 percent confidence limits (Bennett and Franklin, 1954, p. 28)

TABLE 2 – VARIATION OF THE AVERAGE INDENTATION DIAMETER* IN TEST BLOCKS FROM THE SAME LIMESTONE SAMPLE

Sample number	Average diameter – mm Block 1	2	3	4	Average	Standard deviation
K5	1.47	1.44	1.59	1.50	1.500	0.065
K7	1.59	1.57	1.54		1.566	0.025
K14	1.43	1.30	1.35		1.360	0.065
K18	1.74	1.74	1.85	1.79	1.780	0.078
1000	1.68	1.68	1.67		1.677	0.008
1001	1.35	1.35	1.34		1.347	0.007
1008	1.76	1.65	1.72		1.710	0.056
1009	1.28	1.29	1.30		1.290	0.010
1010	1.48	1.40	1.45		1.443	0.041
NF512	1.28	1.34	1.31		1.310	0.036
NF526	1.35	1.35	1.32		1.340	0.017
1007**	1.30	1.25	1.26		1.270	0.026
NF557**	1.32	1.28	1.29	1.29	1.295	0.016

* Average diameter for 5 indentations produced by a fall of 6 cm

** Samples 1007 and NF557 are both siliceous, dolomitic limestones and are included to show that the average indentation diameter of impure carbonate rocks may have variations similar to pure limestones.

TABLE 3 – ELASTIC RECOVERY OF LIMESTONES*

Sample number	Depth of indentation D_m (mm)	$D_c - D_m$ (mm)	Percent
K5a	0.09	0.09	50
K6	0.10	0.08	44
K14	0.06	0.07	54
K18	0.13	0.12	48
1000	0.15	0.05	25
1006	0.10	0.04	29
1010	0.08	0.07	47
NF516	0.13	0.11	46
NF554	0.08	0.06	42

* Initial height of fall is 8 cm in each case.

TABLE 4 - DESCRIPTION OF SAMPLES

Sample number	Location of sample (Nearest town, Illinois)	Geologic unit	Grain* size	Petrographic classification (Folk, 1959)	Remarks
			LIMESTONES		
K14	Alton	St. Louis	Fine	Micrite	Few pyrite grains and calcite veinlets
NF512	Thebes	Girardeau	Fine	Micrite	Quartz and feldspar grains noted
NF526	McClure	St. Clair	Fine	Micrite	Few small spicules
K3	Valmeyer	Salem	Medium	Biosparite	Complex particles, fine and medium crystals
K5	Thebes	Kimmswick	Medium	Biomicrite	Many crystals are cleaved and twinned, partly recrystallized
K5a	Thebes	Kimmswick	Medium	Biomicrite	Bryozoan and Crinoid fragments, partly recrystallized
K6	Marblehead	Burlington	Medium	Biomicrite	Crinoid fragments
K7	Marblehead	Burlington	Medium	Biomicrite	Bryozoan fragments
1000	Anna	Fredonia	Medium	Oosparite	Complex particles
1001	Anna	Fredonia	Medium	Bio-oosparite	Complex particles
1006	Ullin	Harrodsburg	Medium	Biosparite	Bryozoan fragments
1009	Cave in Rock	Fredonia	Medium	Oo-biomicrite	Crinoid fragments
1010	Cave in Rock	Fredonia	Medium	Oosparite	Complex particles
NF511	Elizabethtown	Fredonia	Medium	Biomicrite	Brachiopod fragments
NF519	Jonesboro	Grand Tower	Medium	Biomicrite	Crinoid fragments
NF527	Jonesboro	Harrodsburg	Medium	Biomicrite	Recrystallized with sutured boundaries
I600	Bedford, Indiana	Salem	Medium	Bio-oosparite	Superficial oolite, foraminifera tests
K5b	Thebes	Kimmswick	Coarse	Biomicrite	Notably recrystallized
K18	Jonesboro	Harrodsburg	Coarse	Biosparite	Crinoid fragments with overgrowths
K19	Jonesboro	Harrodsburg	Coarse	Biosparite	Bryozoan fragments
1002	Mill Creek	Harrodsburg	Coarse	Biosparite	Crinoid fragments with overgrowths
1008	Cave in Rock	Fredonia	Coarse	Bio-oosparite	Complex particles
NF516	Mountain Glen	Harrodsburg	Coarse	Biosparite	Microscopic pores common
NF554	Vienna	Glen Dean	Coarse	Biomicrite	Bryozoan fragments
CM1962	New Baden (depth of 2000 feet)	Niagaran	Coarse	Biomicrite	Notably recrystallized
C2740	New Harmony, Indiana (depth of 5464 feet)	Backbone	Coarse	Biomicrite	Notably recrystallized
			DOLOMITES		
61-6a	Manteno	Racine	Fine	Replacement	Even, granoblastic, subhedral grain boundaries, mottled gray and brown
61-7b	Bourbonnais	Waukesha	Fine	Replacement	Even, granoblastic, subhedral grain boundaries
61-8b	Kankakee	Racine	Fine	Replacement	Even, granoblastic, subhedral grain boundaries
62-16-1	Joliet	Joliet	Fine	Replacement	Even, granoblastic, subhedral grain boundaries
62-16-2	Joliet	Kankakee	Fine	Replacement	Even, granoblastic, subhedral grain boundaries
62-20	Grafton	Joliet	Fine	Biogenic	Uneven, subhedral grain boundaries
62-17	Thornton	Racine	Medium	Replacement	Even, granoblastic, anhedral and sutured grain boundaries
62-17c	Thornton	Racine	Medium	Biogenic	Even, granoblastic, subhedral grain boundaries
62-17i	Thornton	Racine	Medium	Biogenic	Crinoidal ghosts, uneven, subhedral grain boundaries
62-21	Elizabeth	Galena	Coarse	Replacement	Even, granoblastic, euhedral

* Grain size classification after Folk (1959, p. 16) which is based on the average size of allochems when present: for limestones <0.063 mm, fine; 0.063 to 1.0 mm, medium; and >0.025 mm, coarse. For dolomites the grain size refers to the median crystal size in which the medium range is 0.063 to 0.250 mm (modified after Folk, 1959, p. 19).

TABLE 5 - PHYSICAL PROPERTIES OF SAMPLES

Sample number	Impact modulus K* $\frac{1}{(cm-sec)}$	Grain** size	Crystal size quartiles (mm) Q_1	M_d	Q_3	Effective porosity (percent)
			LIMESTONES			
1009	275	Medium	.002	.009	.31	0.5
1006	263	Medium	.001	.002	.015	0.3
NF512	262	Fine	.003	.008	.02	0.4
1001	259	Medium	.002	.003	.009	2.5
K14	257	Fine	.002	.003	.004	1.3
NF526	254	Fine	.003	.005	.013	0.05
NF519	236	Medium	.005	.014	.05	0.01
NF511	233	Medium	.002	.008	.02	0.1
NF554	226	Coarse	.003	.005	.02	0.6
1010	223	Medium	.001	.002	.05	2.7
K5	217	Medium	.015	.03	.18	0.2
NF527	211	Medium	.003	.02	.12	2.6
K6	199	Medium	.010	.02	.62	2.1
K7	190	Medium	.013	.02	.09	2.8
K5a	187	Medium	.015	.09	.38	0.6
K5b	184	Coarse	.134	.76	1.23	1.5
1000	164	Medium	.001	.003	.010	8.1
CM1962	164	Coarse	.025	.31	1.23	1.3
1008	160	Coarse	.003	.009	.20	4.6
K19	155	Coarse	.011	.02	.03	8.4
K3	148	Medium	.002	.006	.04	6.6
C2740	143	Coarse	.27	.62	1.11	0.9
K18	136	Coarse	.007	.50	.90	4.7
1002	136	Coarse	.005	.02	.76	6.7
NF516	135	Coarse	.02	.35	.54	1.2
I600	77	Medium	.015	.026	.35	17.3
			DOLOMITES			
62-17	422	Medium	.063	.109	.190	0.4
62-17i	422	Medium	.067	.144	.62	0.7
62-16-1	394	Fine	.029	.051	.088	1.5
61-6a	363	Fine	.036	.051	.077	1.3
62-17c	360	Medium	.069	.154	.268	2.6
61-8b	347	Fine	.030	.044	.063	4.2
62-16-2	347	Medium	.025	.036	.054	5.6
61-7b	279	Medium	.024	.051	.088	5.1
62-20	278	Medium	.026	.036	.051	7.9
62-21	149	Coarse	.21	.33	.47	13.0

* $K = v/r^2\omega$ (equation 4) where r is the radius of indentation (cm), and v impact velocity (cm/sec). All K values listed are computed from results obtained in which v = 108.5 cm/sec (height of fall of indenter equal to 6 cm).

** Same as footnote to grain size in table 4.

REFERENCES

American Society for Testing and Materials, 1961, Standard method of test for toughness of rock, ASTM Designation D3-18, in 1961 Book of Standards, Part 4: ASTM, Philadelphia, p. 613-614.

Brace, W. F., 1960, Behavior of rock salt, limestone, and anhydrite during indentation: Jour. Geophys. Research, v. 65, no. 6, p. 1773-1788.

Brace, W. F., 1961, Dependence of fracture strength of rocks on grain size, in Fourth symposium on rock mechanics: Penn. State Univ. Mineral Industries Experiment Sta. Bull. 76, p. 99-103.

Bennett, C. A., and Franklin, N. L., 1954, Statistical analysis in chemistry and the chemical industry: New York, John Wiley & Sons, Inc., 724 p.

Evans, I., and Pomeroy, C. D., 1958, The strength of cubes of coal in uniaxial compression, in W. H. Walton (ed.), Mechanical properties of non-metallic brittle materials: New York, Interscience Publishers, Inc., p. 5-25.

Fairman, Seibert, and Cutshall, C. S., 1946, Engineering mechanics: New York, John Wiley & Sons, Inc., 267 p.

Finogenov, I. S., 1958, The effects of major natural factors on the hardness of argillaceous carbonate rocks: Izvest. Vysshikh Ucheb. Zaved., Neft i Gaz, v. 1, no. 8, p. 41-46.

Folk, R. L., 1959, Practical petrographic classification of limestones: Am. Assoc. Petroleum Geologists Bull., v. 43, no. 1, p. 1-38.

Friedman, G. M., 1958, Determination of sieve-size distribution from thin-section data for sedimentary petrological studies: Jour. Geology, v. 66, no. 4, p. 394-416.

Gilbert, B. W., 1954, Shore scleroscope hardness tests made on Mohs' scale minerals from talc to quartz inclusive: Univ. Illinois [Urbana] unpublished M. S. thesis.

Greaves, R. H., 1909, The physical interpretation of hardness as measured by the Shore scleroscope: Inst. Civil Eng. [London] Proc., v. 181, no. 4, p. 478-489.

Handin, J. D., Higgs, D. V., Lewis, D. R., and Weyl, P. K., 1957, Effects of gamma radiation on the experimental deformation of calcite and certain rocks: Geol. Soc. America Bull., v. 68, no. 9, p. 1203-1224.

Herbert, E. G., 1929, Cloudburst process of hardness testing and hardening: Am. Soc. Steel Treating Trans., v. 16, no. 1, p. 77-96.

Higgs, D. V., and Handin, J. D., 1959, Experimental deformation of dolomite single crystals: Geol. Soc. America Bull., v. 70, no. 3, p. 245-278.

Maurer, W. C., and Rinehart, J. S., 1960, Impact crater formation in rock: Jour. Appl. Phys., v. 31, no. 7, p. 1247-1252.

Mott, N. F., 1952, Mechanical strength and creep in metals, in W. Shockley, et al. (ed.), Imperfections in nearly perfect crystals: New York, John Wiley & Sons, Inc., p. 173-196.

Obert, Leonard, Windes, S. L., and Duvall, W. I., 1946, Standardized tests for determining the physical properties of mine rock: U. S. Bur. Mines Rept. Inv. 3891, 67 p.

Pavlova, N. N., and Shreiner, L. A., 1961, The rate of loading as influencing the plasticity of marble in indentation tests: Akad. Nauk SSSR, Doklady, v. 137, no. 2, p. 319-322.

Späth, Wilhelm, and Rosner, M. E., 1961, Impact testing of materials: New York, Gordon and Breach, 213 p.

Singh, M. M., and Hartman, H. L., 1961, Hypothesis for the Mechanism of rock failure under impact, in Fourth Symposium on Rock Mechanics: Penn. State Univ. Mineral Industries Experiment Sta. Bull. 76, p. 221-228.

Tabor, D. 1951, The hardness of metals: Oxford, Clarendon Press, 175 p.

Turner, F. J., Griggs, D. T., and Heard, Hugh, 1954, Experimental deformation of calcite crystals: Geol. Soc. America Bull., v. 65, no. 9, p. 883-934.

Whiffin, A. C., 1948, The use of flat-ended projectiles for determining dynamic yield stress, II, Tests on various metallic materials: Royal Soc. [London] Proc., v. 194A, no. 1038, p. 300-322.

Illinois State Geological Survey Circular 345
20 p., 9 figs., 5 tables, 1963

Printed by Authority of State of Illinois, Ch. 127, IRS, Par. 58.25.

CIRCULAR 345

ILLINOIS STATE GEOLOGICAL SURVEY

URBANA